

Supplement of Atmos. Chem. Phys., 18, 103–127, 2018
<https://doi.org/10.5194/acp-18-103-2018-supplement>
© Author(s) 2018. This work is distributed under
the Creative Commons Attribution 3.0 License.



Supplement of

Impact of regional climate change and future emission scenarios on surface O₃ and PM_{2.5} over India

Matthieu Pommier et al.

Correspondence to: Matthieu Pommier (matthieu.pommier@met.no)

The copyright of individual parts of the supplement might differ from the CC BY 3.0 License.

Supplement.

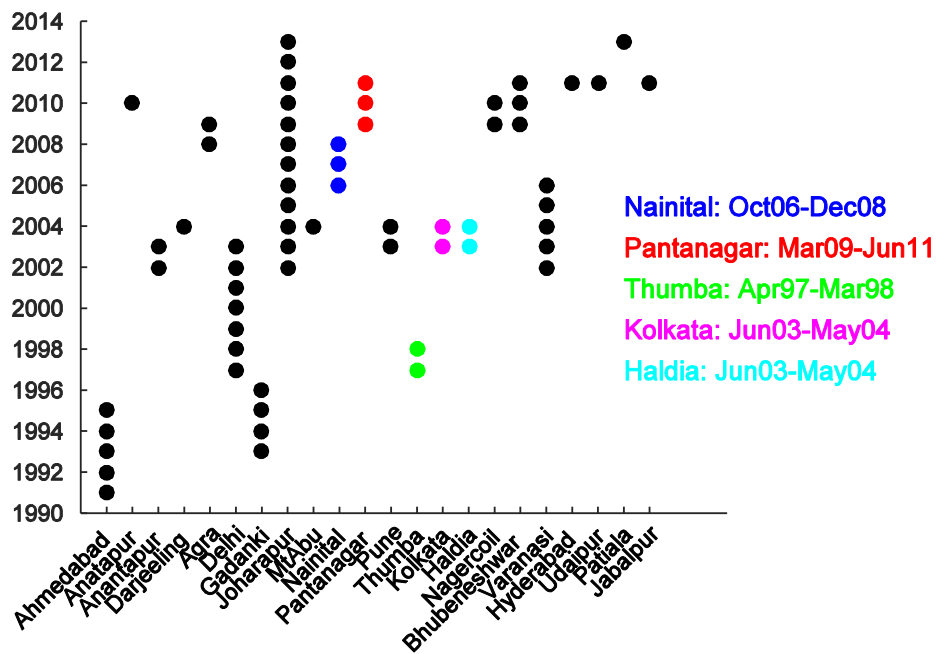


Figure S1. Period of the O₃ measurements for each station in India used in the evaluation. The black dots correspond to the full year and the colored dots represent the partial years. The given period for these partial years with their corresponding station are given in the colored caption.

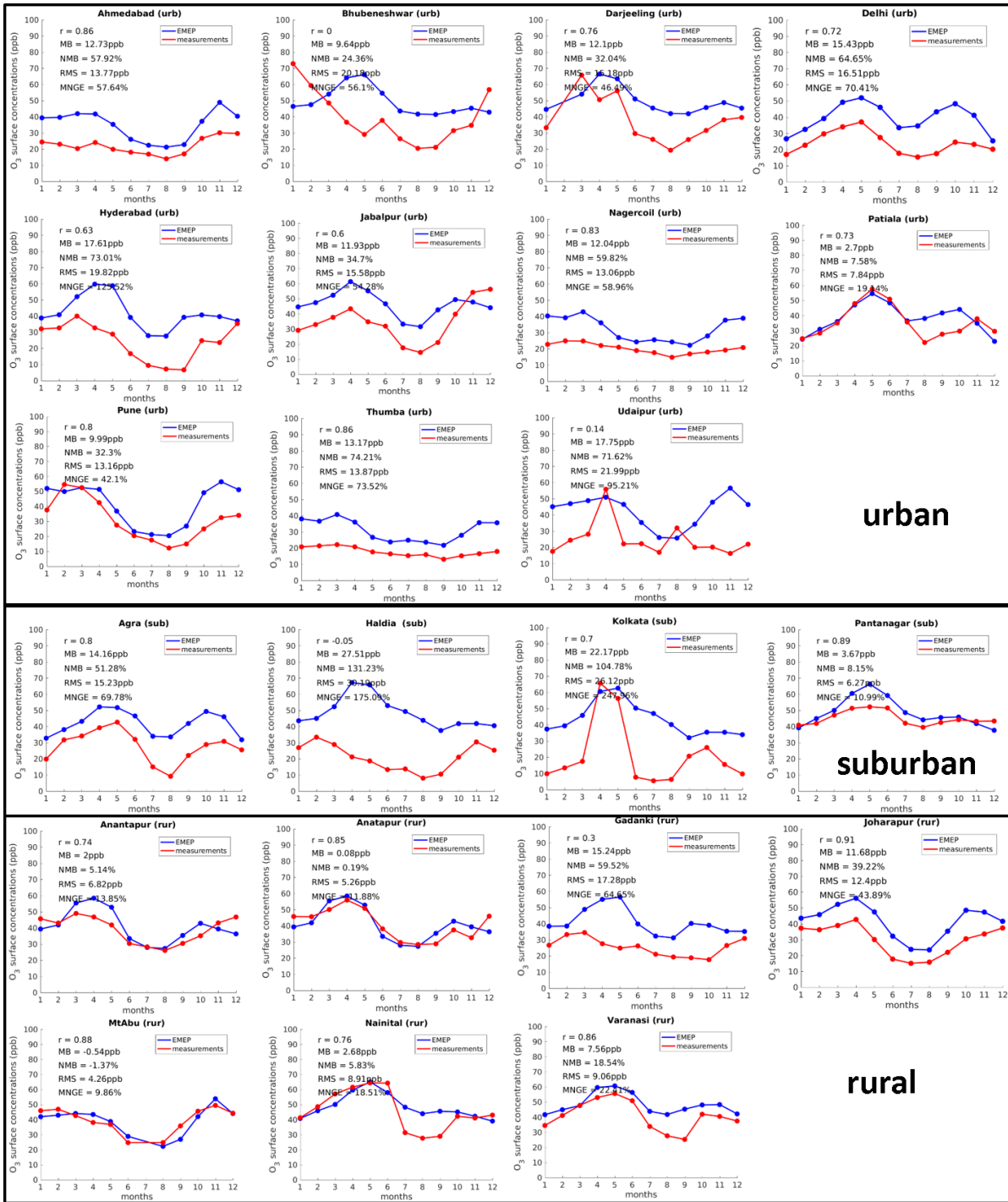


Figure S2. Monthly surface O₃ mean concentrations for all the stations used in Fig. 2. The observations are plotted in red and EMEP (averaged over the period of simulation) in blue. EMEP concentrations are collocated to each station. The correlation coefficient (r), the mean bias (MB), the normalized mean bias (NMB), the Root-Mean-Square (RMS) error, and the mean normalized gross error (MNGE) are provided.

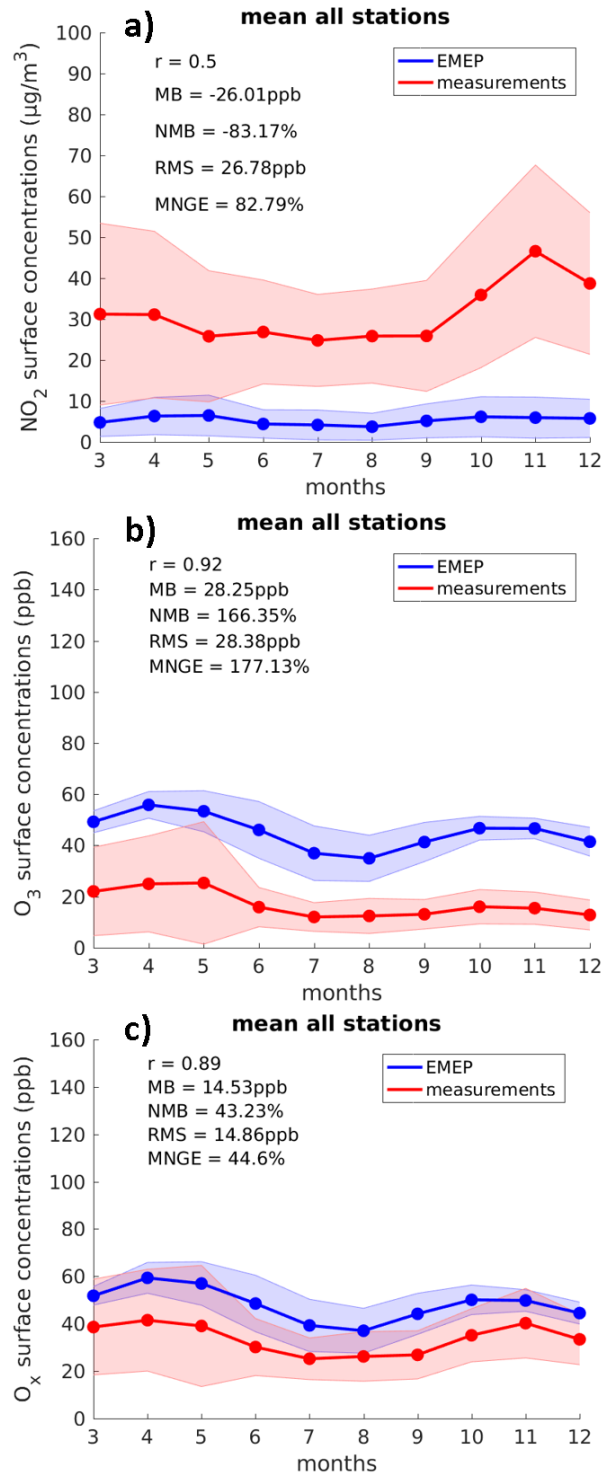


Figure S3. Monthly surface NO₂ (a), O₃ (b) and O_x (c) (O_x = O₃ + NO₂) mean concentrations. The NO₂ and the O₃ concentrations are in µg/m³, and the O_x (converted from the O₃ and NO₂ concentrations) is in ppb. Each plot shows the measurements from the 14 urban stations measuring continuously from March to December 2016 (red) and the result from EMEP for the reference scenario (averaged over the period of simulation) (blue). EMEP concentrations are collocated to each station. The dataset is from <https://openaq.org>. The shade error corresponds to the standard deviation. The correlation coefficient (r), the mean bias (MB), the normalized mean bias (NMB), the Root-Mean-Square (RMS) error, and the mean normalized gross error (MNGE) are provided. January and February were filtered out due to the limited numbers of stations available (no stations measured NO₂ and O₃ from January to December 2016).

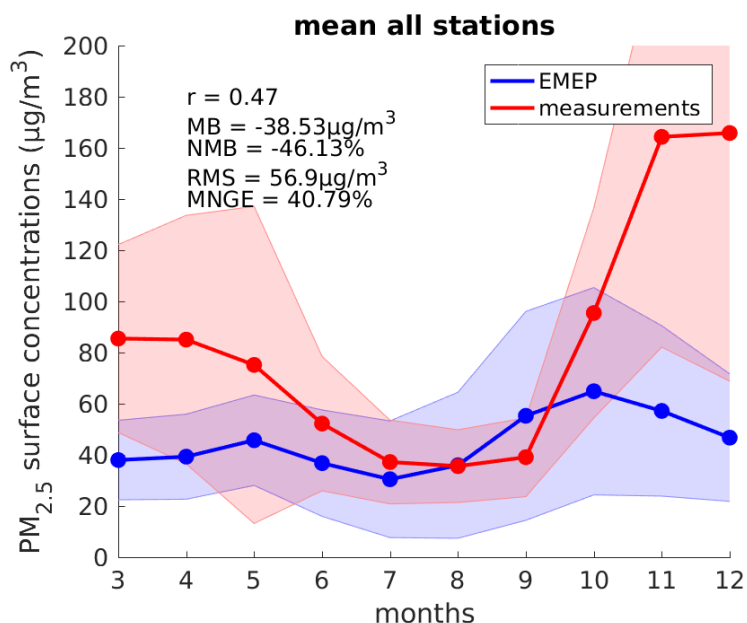


Figure S4. Monthly surface PM_{2.5} mean concentrations in $\mu\text{g}/\text{m}^3$ for 13 urban stations measuring continuously from March to December 2016 (red) and EMEP for the reference scenario (averaged over the period of simulation) (blue). EMEP concentrations are collocated to each station. The dataset is from <https://openaq.org>. The shade error corresponds to the standard deviation. The correlation coefficient (r), the mean bias (MB), the normalized mean bias (NMB), the Root-Mean-Square (RMS) error, and the mean normalized gross error (MNGE) are provided. January and February were filtered out due to the limited numbers of stations available (only 3 stations measured PM_{2.5} from January to December 2016).

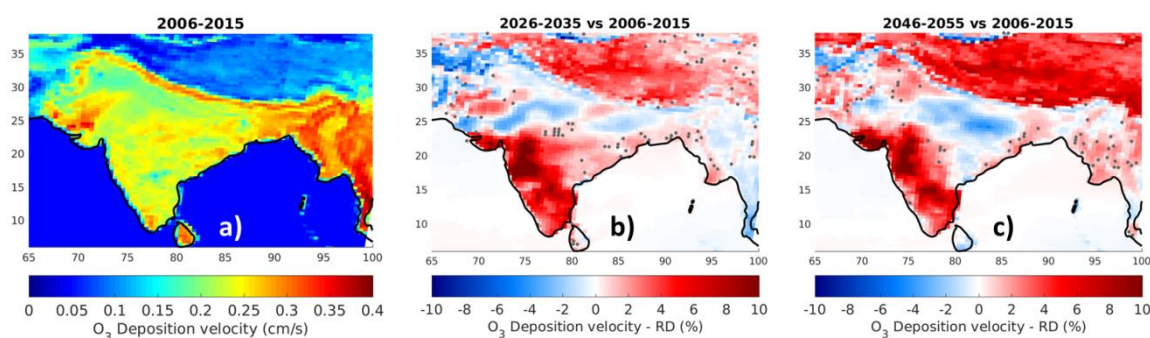


Figure S5. Distribution of O₃ deposition velocity for the reference scenario (a) and distribution of the relative difference in O₃ deposition velocity between the reference scenario and the FC2030 scenario (b) and the FC2050 scenario (c). The relative differences are calculated as: $[(FC - \text{reference}) / \text{reference}] \times 100\%$. Grey dots mark grid points that do not satisfy the 95% level of significance.

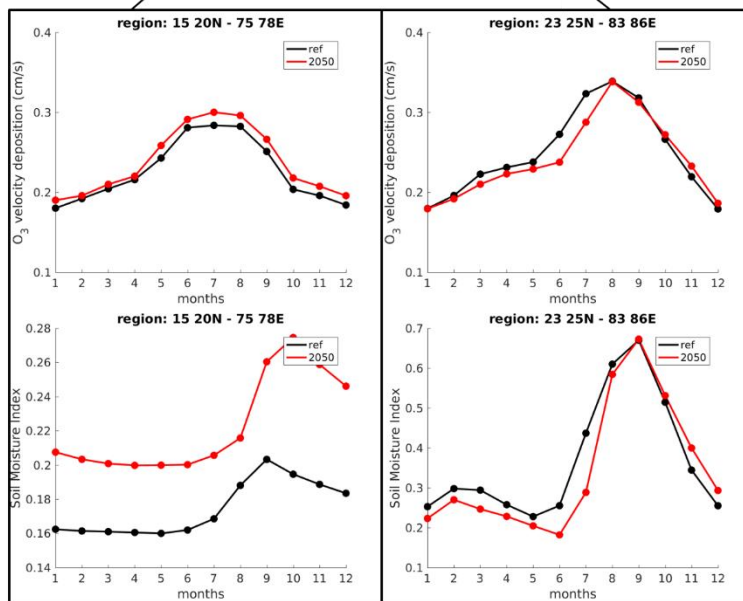
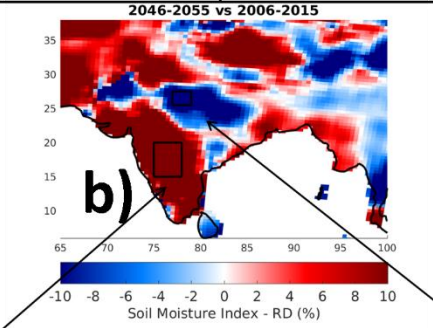
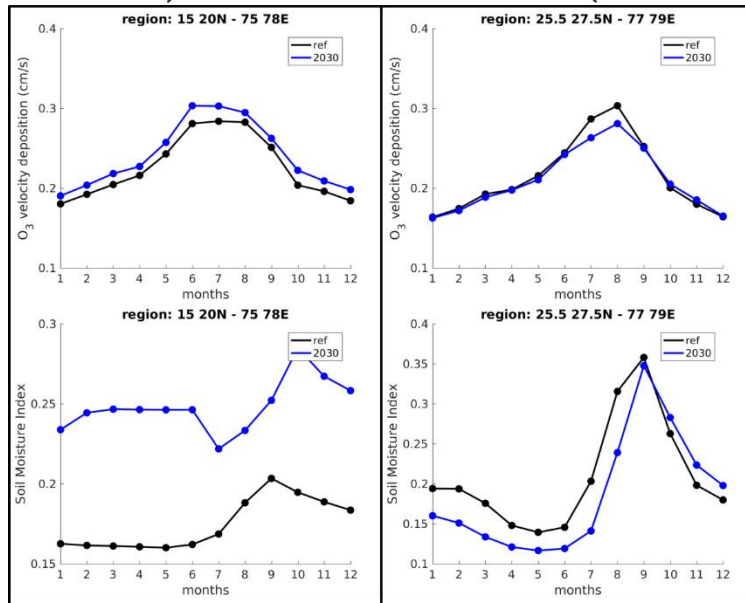
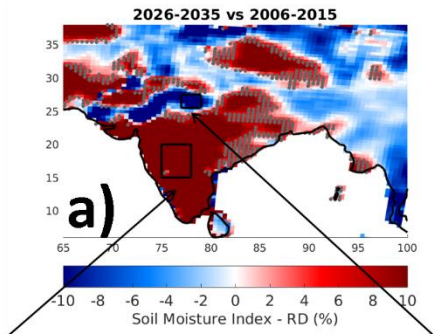


Figure S6. Distribution of the relative difference in soil moisture index between the reference scenario and the FC scenarios (top panel), time-series of the monthly O₃ deposition velocity (middle panels) and time-series of the monthly soil moisture index (bottom panels) for both regions plotted on the maps. The relative difference is calculated as: $([FC - \text{reference}] / \text{reference}) \times 100\%$. The results for the FC2030 scenario are plotted in (a) and for the FC2050 scenario are plotted in (b). The values for the reference scenario are plotted in black and those for the FC2030 scenario in blue and for the FC2050 scenario in red. On the maps, grey dots mark grid points that do not satisfy the 95% level of significance.

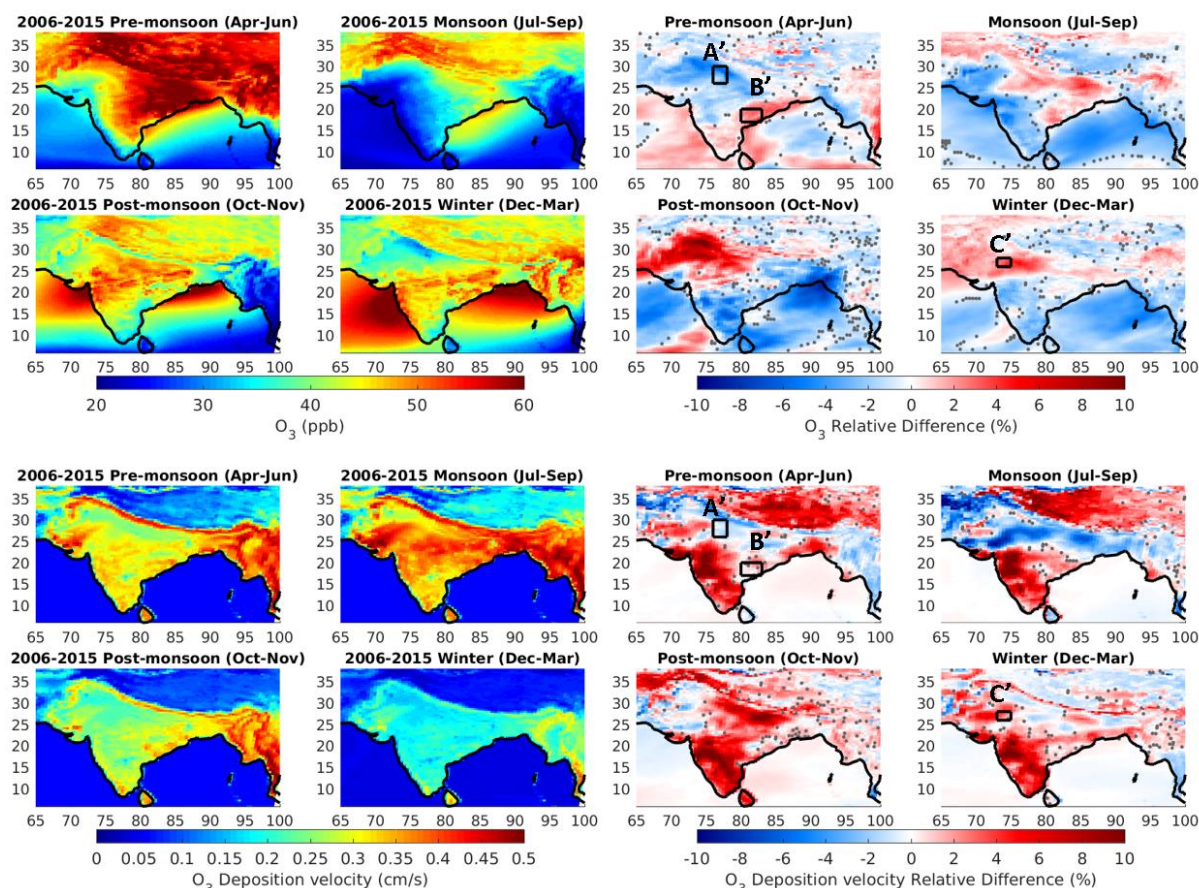


Figure S7. Seasonal distribution of O₃ and relative difference between the reference scenario and the FC2030 scenario (top panels), seasonal distribution of O₃ deposition velocity and relative difference between the reference scenario and the FC2030 scenario (bottom panels). The relative differences are calculated as: $([FC2030 - \text{reference}] / \text{reference}) \times 100\%$. Regions discussed in the text are labelled on the distributions of relative difference. Grey dots mark grid points that do not satisfy the 95% level of significance.

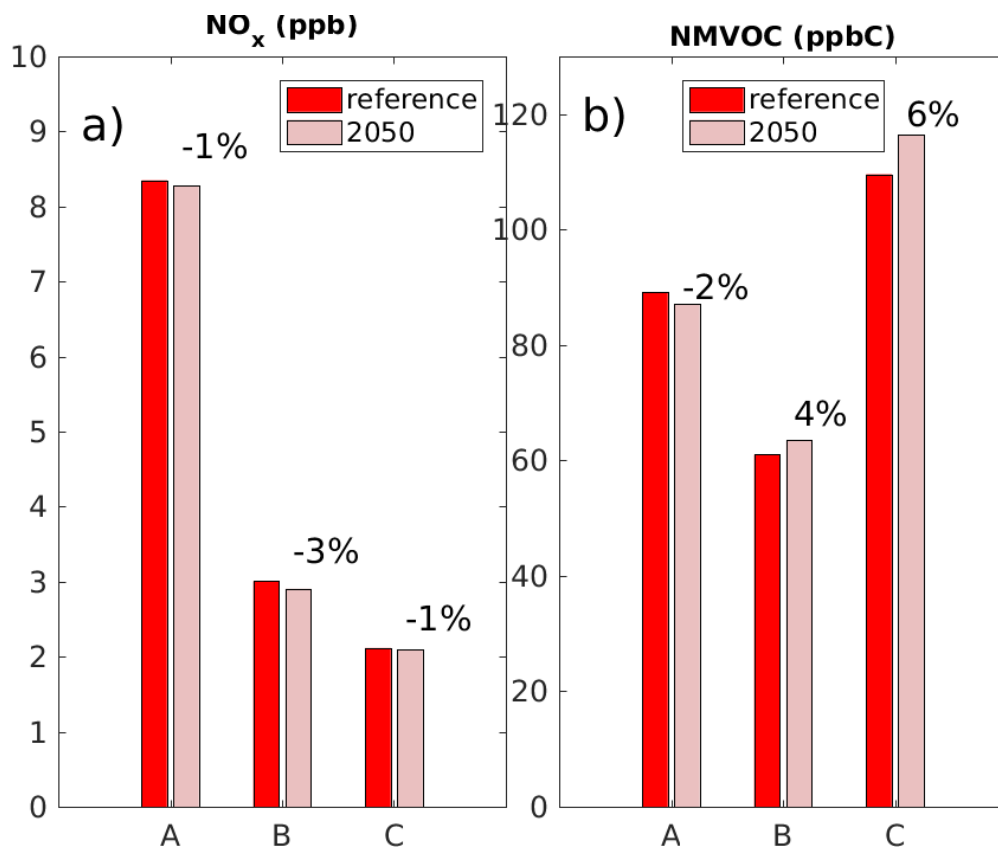


Figure S8. Surface mixing ratios of NO_x (a) and NMVOC (b) for the reference scenario (red) and the FC2050 scenario (pink) over the three selected regions during their corresponding season, highlighted in Fig. 8. The relative differences between both scenarios over each region are also indicated. The relative differences are calculated as: $[(FC2050 - reference) / reference] \times 100\%$.

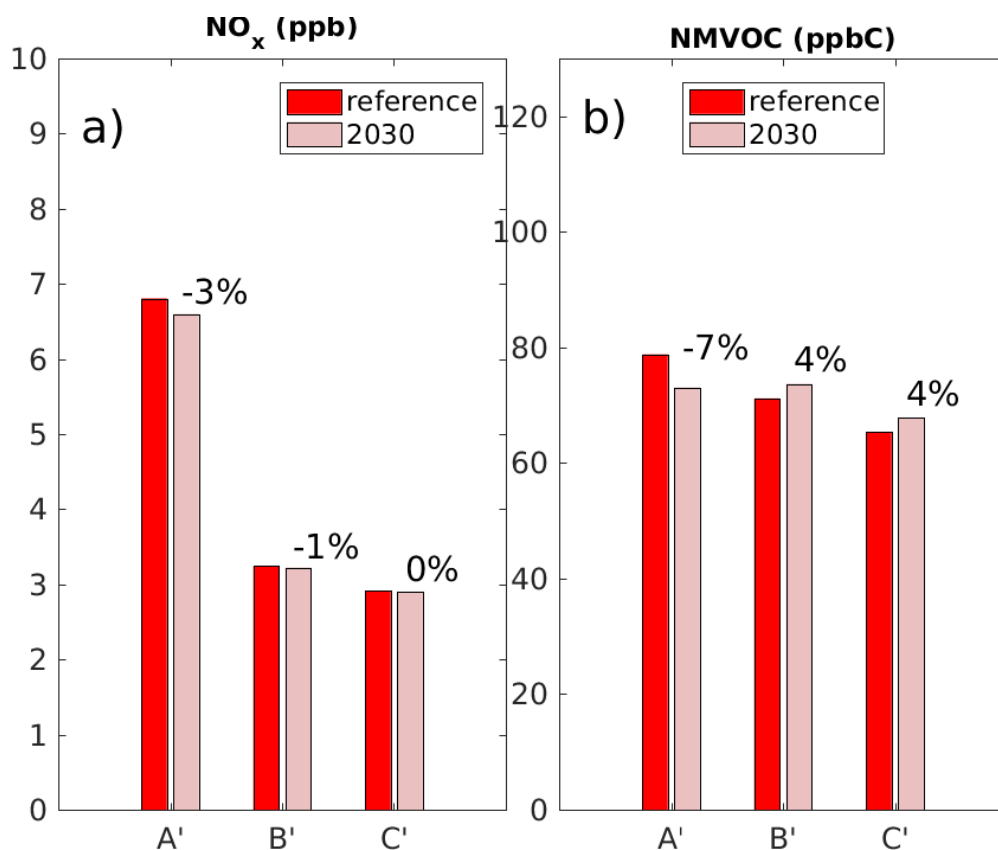


Figure S9. Surface mixing ratios of NO_x (a) and NMVOC (b) for the reference scenario (red) and the FC2030 scenario (pink) over the three selected regions during their corresponding season, highlighted in Fig.S7. The relative differences between both scenarios over each region are also indicated. The relative differences are calculated as: $[(FC2030 - \text{reference}] / \text{reference}] \times 100\%$.

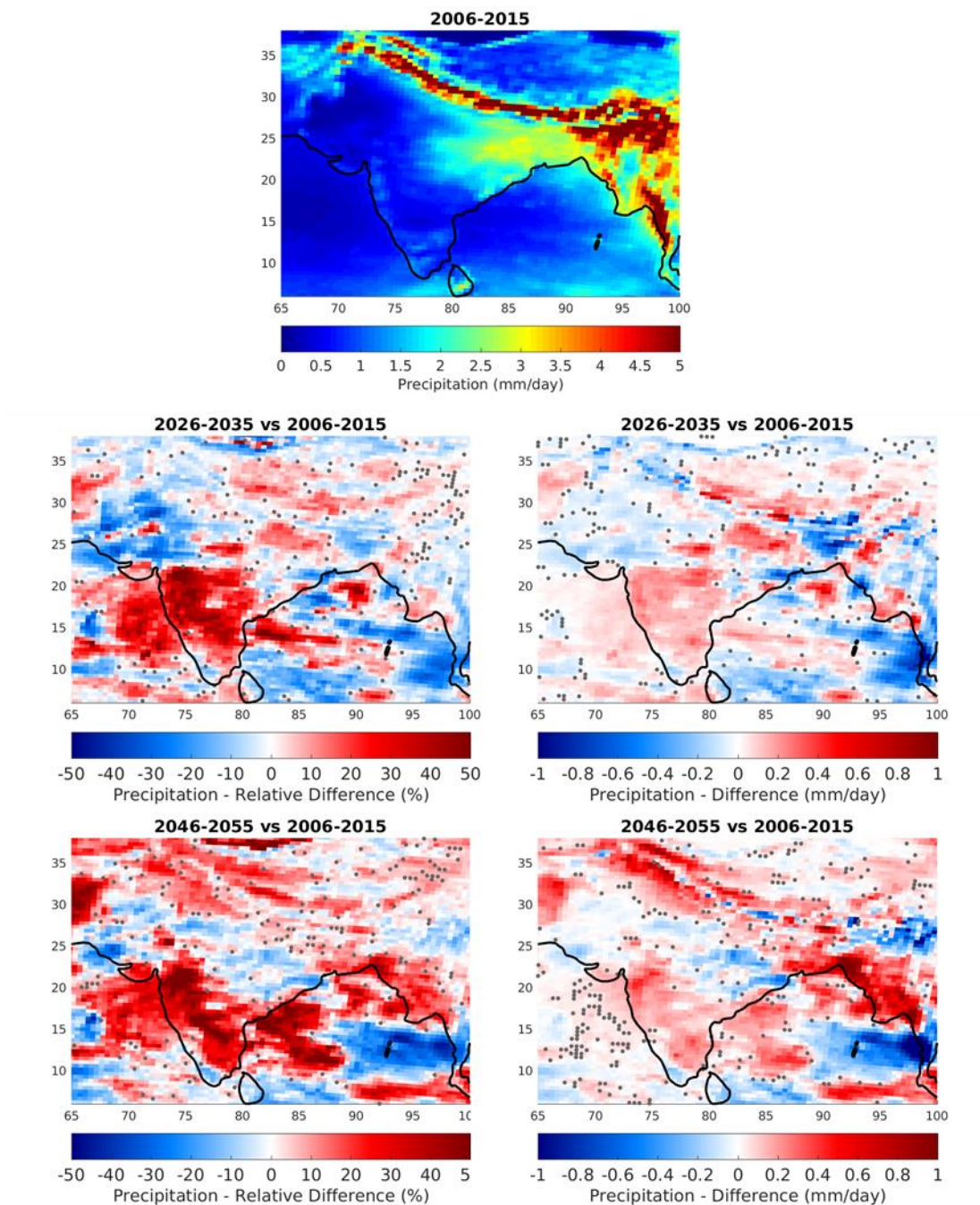


Figure S10. Distribution of precipitation (in mm/day) for the reference scenario (top panel), distribution of the relative difference and absolute difference in precipitation between the reference scenario and the FC2030 scenario (middle panels) and the FC2050 scenario (bottom panels). The relative differences are calculated as: $[(FC - \text{reference}] / \text{reference}] \times 100\%$, and the absolute differences as: $[FC - \text{reference}]$. Grey dots mark grid points that do not satisfy the 95% level of significance.

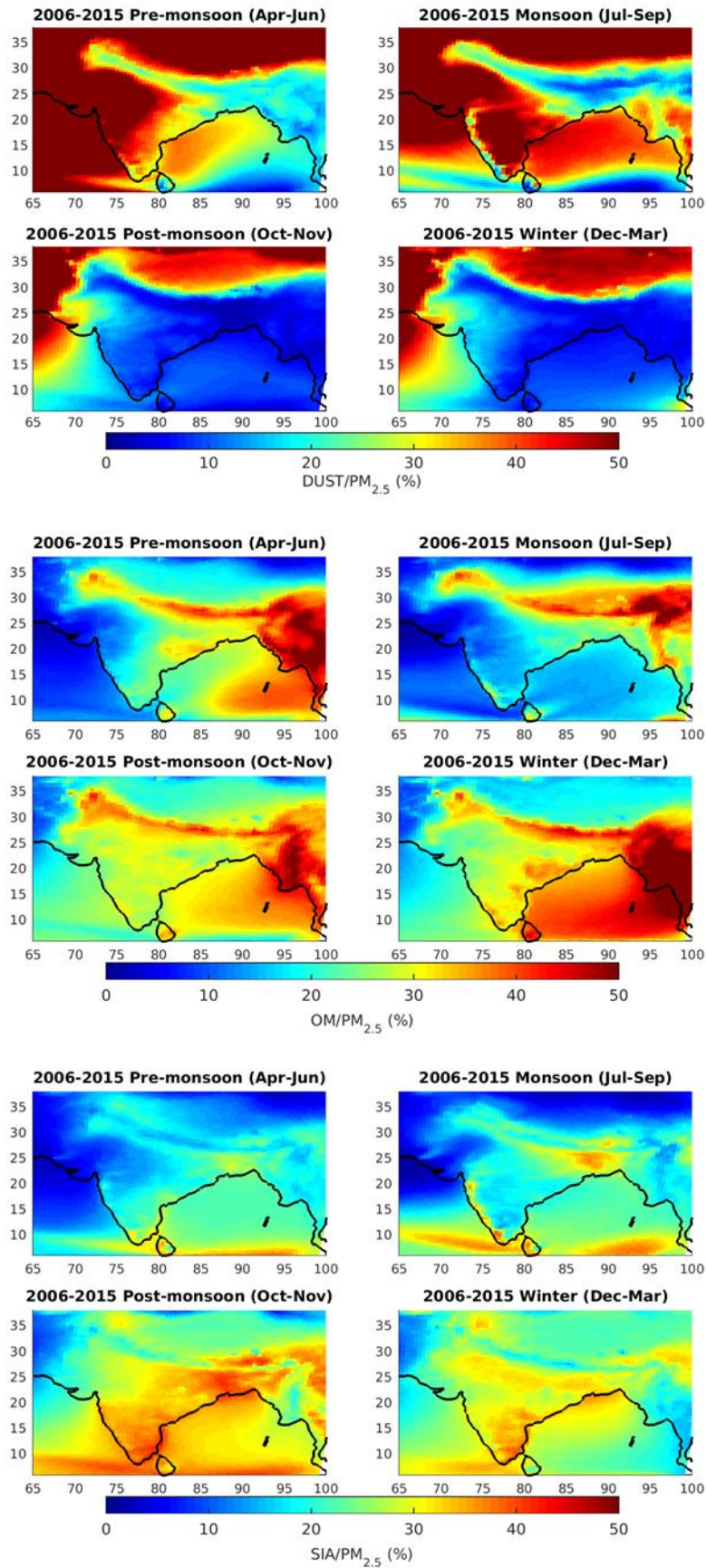


Figure S11. Seasonal distribution of ratio of dust (top panels), OM (mid-panels) and SIA (bottom panels) on surface $PM_{2.5}$ concentrations for the reference scenario.

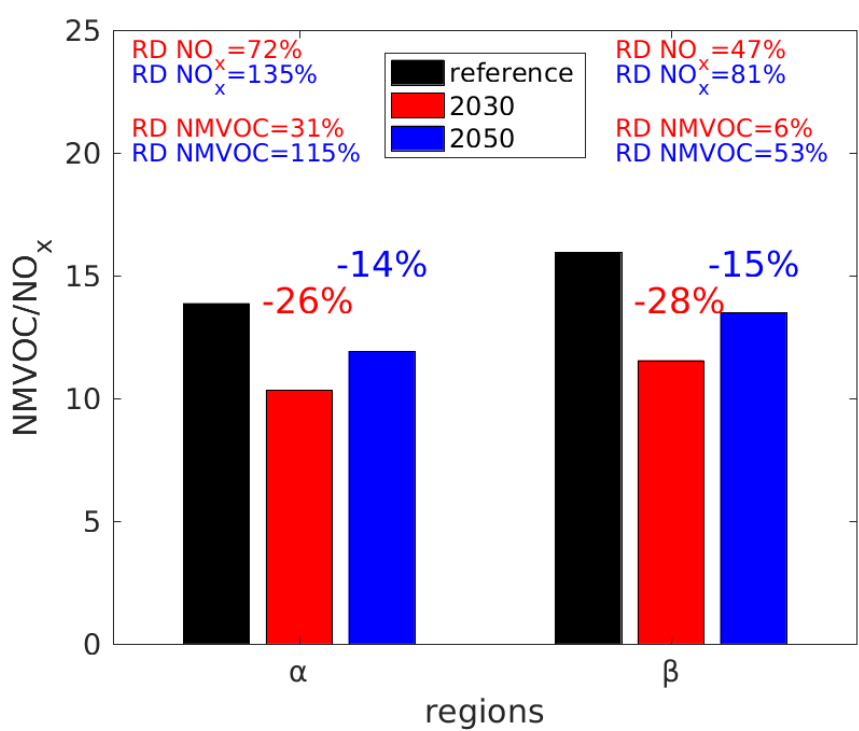


Figure S12. Mean NMVOC/NO_x ratio (ppbC/ppb) over region (α) during the monsoon and over region (β) in winter as shown in Fig. 12. The ratio for the reference scenario is plotted in black, for the FCE2030 scenario in red and for the FCE2050 scenario in blue, for both regions. The mean relative difference with respect to value in the reference scenario is written with the corresponding color. The mean relative difference for the NO_x and NMVOC are also indicated.

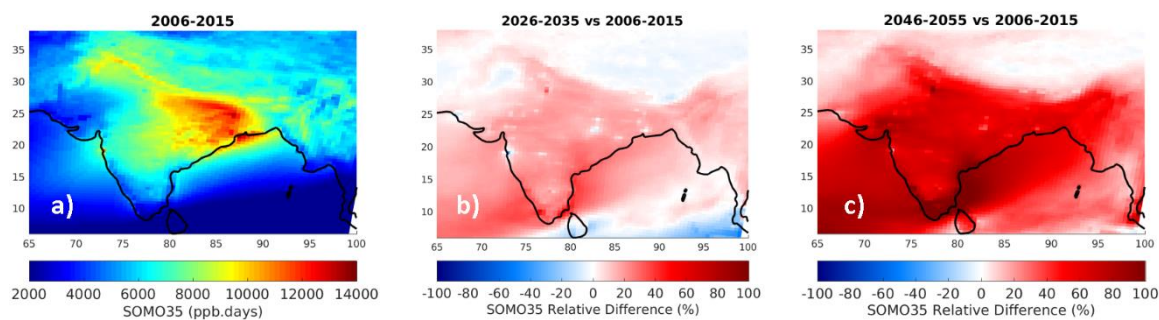


Figure S13. Distribution of SOMO35 levels for the reference scenario (a), and of the relative difference in SOMO35 between the reference scenario and the FCE2030 scenario (b) and the FCE2050 scenario (c).

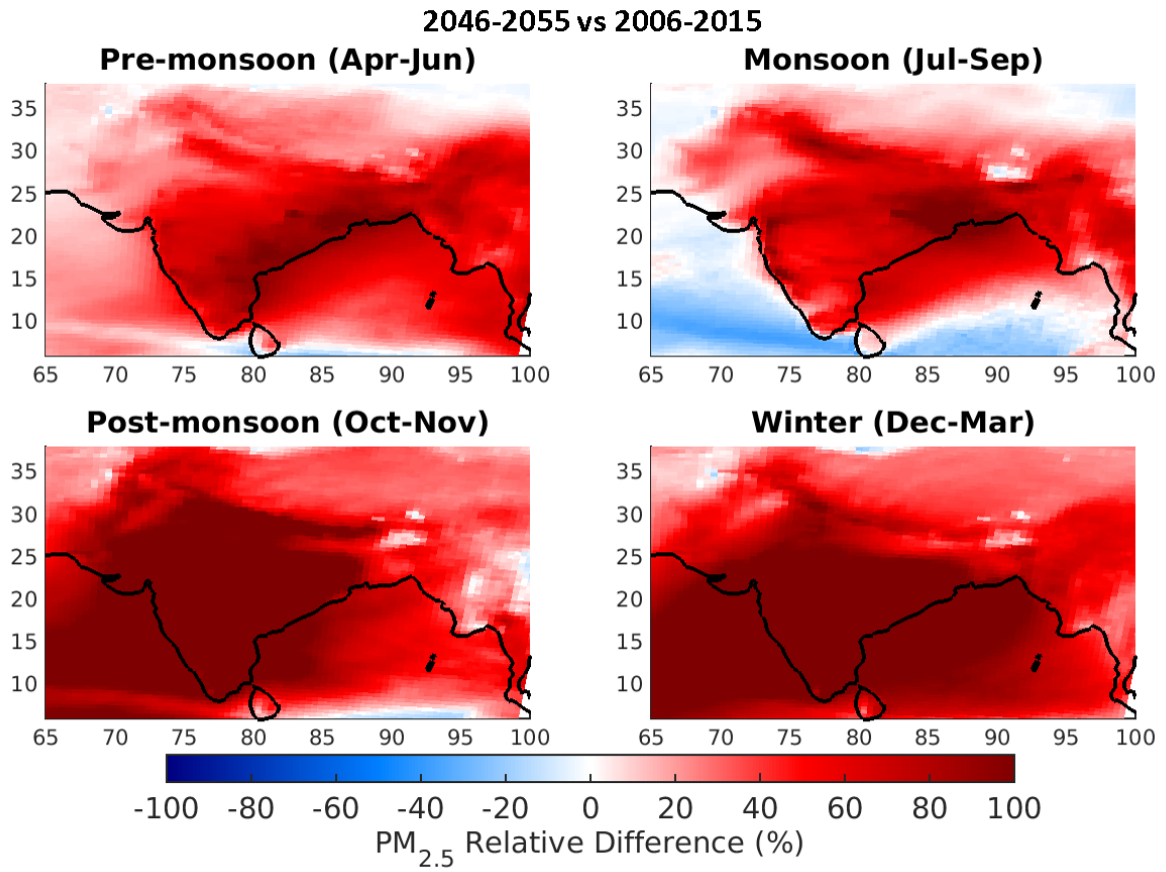


Figure S14. Seasonal distribution of the relative difference in surface PM_{2.5} between the reference scenario and the FCE2050 scenario. The relative differences are calculated as: $([FCE2050 - \text{reference}] / \text{reference}) \times 100\%$.

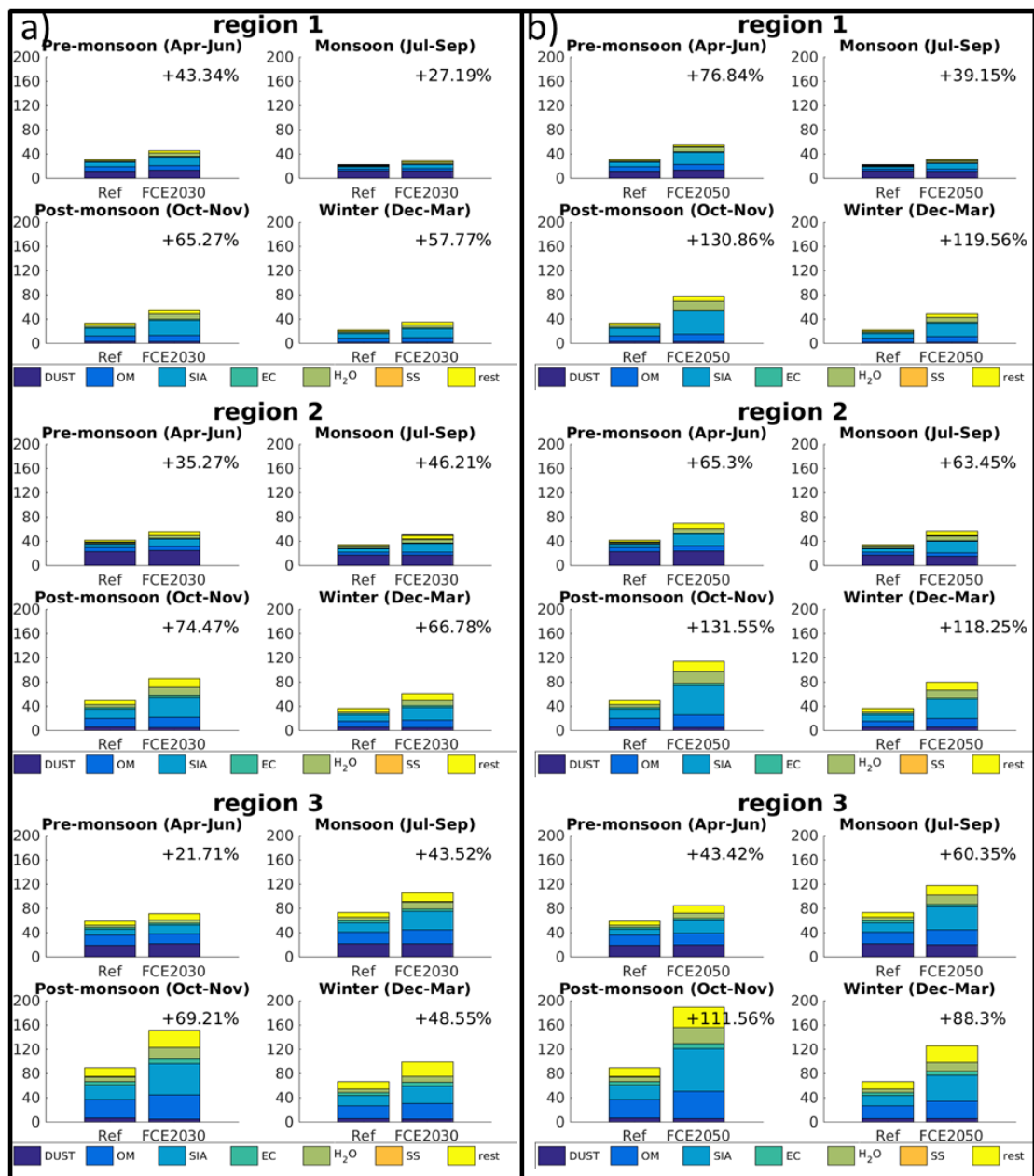


Figure S15. Seasonal composition of $PM_{2.5}$ (in $\mu g/m^3$) for the three regions highlighted by black boxes in Fig. 10 for the reference and the FCE2030 (a), and FCE2050 (b) scenarios. The black percent corresponds to the relative difference in $PM_{2.5}$ between the FCE scenarios and the reference scenario for each region.